# Facilitate sEMG-based Human-machine Interaction through Channel Optimisation

Zheng Wang
College of Computer Science & Technology, Zhejiang University of Technology
288 Liuhe Rd, Hangzhou, 310023 , China
Zheng.Wang1@myport.ac.uk

Yinfeng Fang
College of Telecommunication, Hangzhou Dianzi University
1158, No.2 Avenue, Xiasha, Hangzhou, 310018, China
yinfeng.fang@hdu.edu.cn

Honghai Liu
Intelligent Systems and Biomedical Robotics Group, School of Computing
University of Portsmouth, Portsmouth, PO1 3HE, UK
honghai.liu@port.ac.uk
School of Mechanical Engineering, Shanghai Jiao Tong University
Shanghai, 200240, China
hnllyu@sjtu.edu.cn

Electromyoraphy (EMG) has been widely accepted to interact with prosthetic hands, but still limited to using few channels for the control of few degrees of freedom. The use of more channels can improve the controllability, but it also increases system's complexity and reduces its wearability. It is yet clear if optimisely placing the EMG channel could provide a feasible solution to this challenge. This study customised a genetic algorithm to optimise the number of channel and its position on the forearm in inter-day hand gesture recognition scenario. Our experimental results demonstrate that optimally selected fourteen channels out of sixteen can reach a peak inter-day hand gesture recognition accuracy at 72.3%, and optimally selecting nine and eleven channels would reduce the performance by 3% and 10%. The cross-validation results also demonstrate that the optimally selected EMG channels from five subjects also works on the rest subjects, improving the accuracies by 3.09% and 4.5% in nine- and eleven-channel combination, respectively. In sum, this study demonstrates the feasibility of channel reduction through genetic algorithm, and preliminary proves the significance of EMG channel optimisation for human-machine interaction.

Keywords: Hand motion; electromyography; pattern recognition; genetic algorithm;

## 1. Introduction

Surface electromyography (sEMG) is the recording of the electrical potentials around the electrodes on skin surface. These potentials are discharged due to muscular contraction under the skin surface. The initial use of sEMG as a human-machine interface (HMI) is to interact with prostheses by patients after amputation. Because sEMG signal is closely linked to neural signals from the brain [1], sEMG-based prosthetic control can be intuitive without the requirement of intensive user training procedure. Recent studies also attempt to use sEMG as a general HMI to control external devices, such as robotic arms, tablets, unmanned aerial vehicle, and etc. Although EMG-based HMI (MyoHMI) has intensively studied for several decades [2,3,4,5,6,7], it is still not robust enough, especially when more discrete commands need to be decoded from a few channels.

Electrode configuration, involving sEMG channel number and electrode distribution on the skin surface, is closely related to the efficient and effective of a MyoHMI. On the one hand, the channel number should be reduced to obtain a cost-efficient system, and thus the relation between the number of sEMG channel and its recognition accuracy need to be investigated. On the other hand, the electrode positioning strategy need to be optimised under a certain number of sEMG channel to achieve higher performance on hand gesture recognition. With the development of bio-signal sensing technology and compact integrated circuits, researchers tend to apply high density EMG for the study of myoelectric control [8,9,10], however it is not likely to promote MyoHMIs to be a portable device.

It is hard to identify how many channels are most suitable for myoelectric control that balances the cost and its performance due to different experimental setups. Taking myo-prosthesis as an example, although sufficient evidence has been show that the increase of sEMG channels can provide a more natural and reliable control [11,12], commercially successfully myo-prosthesis still employs two bi-polar EMG electrodes on forearm extensor and flexor. Space limitation, power consumption and real-time performance limits the use of larger number of sEMG channels [13,14,15]. As such, on the one hand, researchers tends to carry out experiment with increasing sEMG channels. On the other hand, a reduction in the number of electrodes, without compromising accuracy, attracts great attention to simplify system requirement [16]. Young et al.[17] show that four to six channels were sufficient for pattern recognition control, while Li, et al. show that use of 6 optimally-placed electrodes for 12 electrodes only reduced this accuracy by 1.6%. Also, Huang et al. [18] demonstrate that 12 selected bipolar electrodes can obtain a similar classification accuracy (1.2% drops) comparing to using the entire HD electrode complement in a TMR application.

The electrode configuration approach can be generally divide into three groups: muscle-targeted (MT) layout, low-density (LD) layout, and high-density (HD) layout[19]. MT layout requires the precise positions of muscles, and adhere electrodes on the belly of the muscles, and thus it may require somewhat anatomical

knowledge. Several examples of this layout can be found in[20,21,22]. LD layout arranges the electrodes on the skin surface regardless the accurate location of muscles, and these electrodes are normally evenly placed on the skin, also termed as uniform electrode positioning strategy[23]. The channel number of LD layout usually ranges from two to sixteen. For instance, six bipolar electrodes were distributed uniformly at 1/3 of the distance from elbow to wrist[24]. HD layout is a noninvasive technique that collects myoelectric signals from many closely spaced electrodes[25] (The inter-distance can be less than five mm or ten mm), which would allow to better exploit the spatial information across the muscles, and therefore can be more useful for the study of complex dynamic tasks in the free space and with a greater number of DOFs[14]. HD-EMG are usually related to energy maps that illustrates which electrode locations experience strong myoelectric activity during each task performed, and these maps can be examined to determine if distinguishable muscle activation patterns are produced for different tasks for each subject[11]. Since HD EMG contains sufficient information at an instance, deep learning approaches has been applied to decode hand gestures in the recent years[9,10]. However, the use of a large number of EMG electrodes hinders the application of HD EMG. In sum, LD layout is a more suitable choice to fulfil a consumable and portable MyoHMI in the comparison with MT layout that is troublesome in wearing electrode and HD layout that is expensive and complex.

To the best of our knowledge, it is the first study to optimise electrode/channel configuration via artificial algorithms. Rather than channel optimisation that is physically linked to the electrode positioning strategy, related studies have tried to identify most efficient sEMG feature. Dalin et al.[26] adopted a bacterial memetic algorithm as the feature selection strategy for sEMG based hand motion recognition, and a promising trade-off between the reduction of computation cost and the comprising in recognition rate has been seen in the experiments. Oskoei et al.[27] adopts genetic algorithms to explore the subset of sEMG feature in a 4-channel system, and improved myoelectric signal classification.

The remaining of this paper is organised as follows. Section ?? summarises related works on sEMG electrode configuration. Section 2 presents the sEMG data acquisition setups, and the technologies on sEMG signal processing, feature extraction and classification. Section 2.6 establishes the genetic algorithm based model for sEMG channels optimisation. Section 3 and 4 disclose the experimental results with discussion. Section 5 concludes the paper with future work.

## 2. Materials and methods

### 2.1. Subjects

Six able-bodied subjects (two females, four males; age range: 22 - 31 years) volunteered for the experiment. The subjects were all normally limbed with no neurological or muscular disorders. The data acquisition was approved by the ethics committee of University of Portsmouth and written informed consent was obtained


Figure 1. The experimental setup for sEMG data collection.

from all subjects.

### 2.2. Experimental Setup

The sEMG acquisition system customised by the Intelligent System and Biomedical Robotics Group of University of Portsmouth[28,29], as displayed in Fig. 1. The system mainly consisted of three components: an electrode sleeve (Fig. 1-1), a 16-channel sEMG signal amplifier, (Fig. 1-2), and a signal acquisition software (Fig. 1-3). The electrode sleeve was designed to embed 18 dry electrodes on a flexible fabric, forming 16 bi-polar sEMG channels. An empty sleeve was employed to cover the electrode sleeve to mitigate movement artefacts. Two of the eighteen electrodes were grounded and the remaining sixteen electrodes formed 16 bi-polar sEMG channels by sharing each electrode with two neighbouring channels[30]. Fig. 10 demonstrates the sEMG channel position against the forearm anatomy. The sEMG signal was enhanced by the amplifier with the gain of 1000, and sampled at 1000 Hz. Besides, the amplifier also depressed the frequent components beyond the range of 20-500 Hz and 50 Hz (power line noise frequency) for each individual sEMG channel. A sEMG signal acquisition software was developed to synchronise, record and process the sEMG signal in a visualised manner.

### 2.3. Data Recording Protocol

In the experimental protocol, all subjects were informed to wear the electrode sleeve with a rough reference (i.e. two ground electrodes placed on the ventral side of the forearm and pulled the sleeve right above the elbow) without the use of electrode location markers. After wearing the sleeve, the experimental procedure were introduced to the subjects in a face-to-face teaching manner in the first acquisition day.

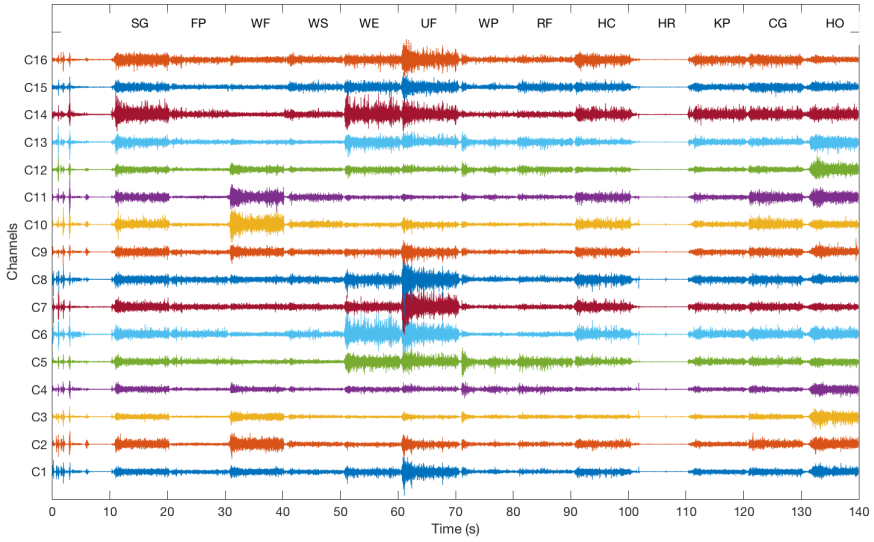


Figure 2. Sixteen channels of sEMG signal

During data capturing, subjects sat comfortably in an office chair and put the right elbow on the desktop, as seen in Fig. 1. There was no restricted rule on the elbow joint angle or the force effort on the gestures. Each subject was required to implement two sessions each day with an interval of about half an hour, and recorded for ten days. For each session, subjects were required to follow the cue signals to perform hand motions sequentially in a random order, and each motion lasted for ten seconds. These motions including Hand Rest ($HR$), Hand Closed ($HC$), Hand Open ($HO$), Wrist Flexion ($WF$), Wrist Extension ($WE$), Wrist Pronation ($WP$), Wrist Supination ($WS$), Ulnar Flexion ($UF$), Radial Flexion ($RF$), Fine Pinch ($FP$), key pitch ($KP$), spherical grasp ($SG$) and cylindrical grasp ($CG$). Fig. 2 demonstrates 16 channels of sEMG signal during a 140 second recording period (i.e. a session).

## 2.4. Data Segmentation and Feature Extraction

### 2.4.1. Sliding window for feature extraction

Sliding window functions to segment EMG signals and estimate the intended motions from each window by continuous classification[32]. In every window, sEMG features can be obtained from multiple EMG channels. Fig. 3 illustrates the incremental windows, where one channel of EMG signal is segmented by sliding windows, where $w$ is the window length; $t$ is the incremental interval and $\tau$ is the processing delay. Within a period of $t$, classification decision needs be made to meet the real-time requirement, $\tau \leq t$. These parameters somewhat affect the performance of a MyoMHI, as discussed below.

- Window length ($w$). It determines the amount of data being used in the feature extraction and classification. A larger amount of data will contribute

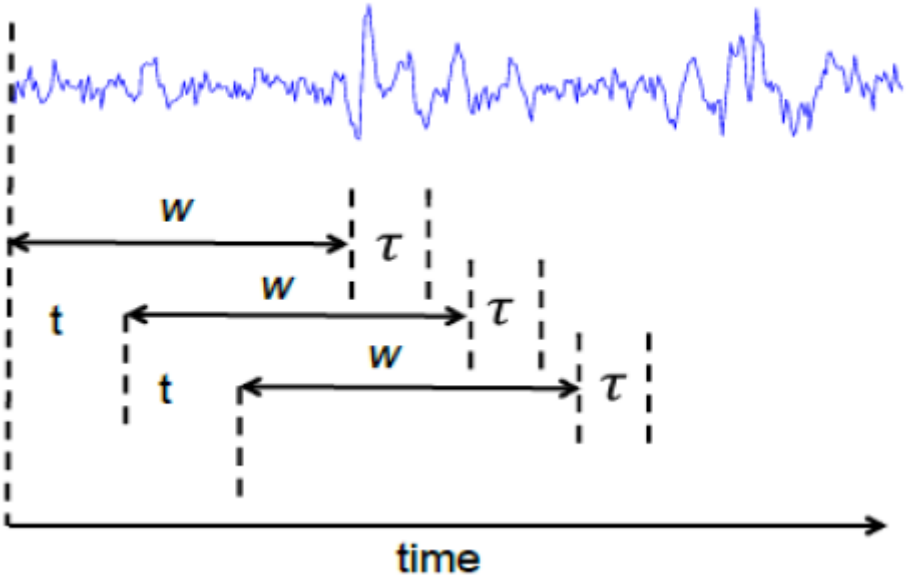


Figure 3. Slinding winding for feature extraction, adopted from[31]

to a lower statistical variance of features, and therefore, achieve greater classification accuracy[32]. However, it would induce a longer processing delay.

- Incremental interval (*t*). It determines the bounds allowing the control system to extract feature vectors as well as generate a classification decision. Thus, the computing time of any algorithm should satisfy this demand.

2.4.2 Feature extraction

The most prevalent Hudgins' TD features, including Mean Absolute Value (MAV), Waveform Length (WL), Zero Crossing (ZC) and Slope Sign Changes (SSC), in combination with 4-th order autoregressive coefficients (AR4) are adopted as the baseline feature options. The definition of these sEMG features is defined as below, where *N* is the sliding window size, and $x_i$ is an instant sEMG value at the time point *i*.

- MAV is an average of absolute value in the segment, which relatively accurately illustrates the change trend of the absolute value in sEMG signal. MAV could be defined as

$$MAV = \frac{1}{N}\sum_{i=1}^{N}|x_i|. \quad (1)$$

- WL is the cumulative length of the waveform of an EMG. It can be formulated as

$$WL = \sum_{i=1}^{N-1}|x_{i+1} - x_i|. \quad (2)$$

- ZC is the number of times that a signal crosses zero, which is somewhat associated with the frequency of EMG signals.

$$ZC = \sum_{i=1}^{N-1} \text{sgn}(-x_i x_{i+1}), \tag{3}$$

where

$$\text{sgn}(x) = \begin{cases} 1 & x > \varepsilon \\ 0 & x \leqslant \varepsilon \end{cases} \tag{4}$$

and $\varepsilon$ is the threshold to avoid low-level noises.

- SSC provides another measure of frequency content measuring the number of times the slope of the waveform changes sign.

$$SSC = \sum_{i=2}^{N-1} f(x_{i-1}, x_i, x_{i+1}), \tag{5}$$

where

$$f(x_{i-1}, x_i, x_{i+1}) = \begin{cases} 1 & (x_{i+1} - x_i)(x_{i-1} - x_i) > 0 \; AND \\ & (|x_{k+1} - x_k| > \varepsilon \; OR \; |x_{k-1} - x_k| > \varepsilon) \\ 0 & else \end{cases} \tag{6}$$

- Auto-regressive (AR) coefficients are usually used as features of EMG signals. AR model presents that an EMG signal can be considered as a linear combination of previous EMG signal ($x_{k-i}$) plus a white noise error term ($e_i$). It is defined as

$$x_k = \sum_{i}^{p} a_i x_{k-i} + e_k, \tag{7}$$

where $p$ is the order of AR model, and $a_i$ is the coefficients that are utilised as EMG features.

In the current study, the parameters of the $w$ and $t$ are set to 256 ms and 64 ms, respectively. Since the sEMG signal is captured at the sampling frequency 1000 Hz, 256 ms sEMG signal contains 256 sampling points (i.e. $N = 256$). The threshold $\varepsilon$ for the calculation of ZC and SSC is set to 8 mv. Each gesture maintains for ten seconds, which allows the sEMG signal within ten seconds containing both transient and steady signal. The transient signals are excluded by removing the signals of the first five seconds.

After removing transient signal, the sEMG feature (128 dimensions) are extracted with sliding window segmentation. Eventually, this study obtains 1950 samples in one day, and 150 samples per gesture. In the following test, the fitness value of the genetic algorithm is the averaged classification accuracy in 10-fold cross validation, where the samples from one of ten days are selected in turn for test, and the rest for classification training.

### 2.5. LDA Classifier

Linear discriminant analysis (LDA) based classification approach is widely accepted in sEMG signal classification, because it can provide robust classification result against the sEMG interferences. LDA assumes data of each class follows multivariate Gaussian distribution with homoscedastic covariance. The probability density function $P(\mathbf{x}|i)$ of the class $i$ is defined as:

$$P(\mathbf{x}|i) = \frac{1}{(2\pi)^{|\mathbf{x}|/2}|\Sigma_i|^{1/2}} \exp(-\frac{1}{2}(\mathbf{x}-\mu_i)^T\Sigma_i^{-1}(\mathbf{x}-\mu_i))) \tag{8}$$

where $|\mathbf{x}|$ is the dimension of the vector $\mathbf{x}$, $\mu_i$ and $\Sigma_i$ are the mean vector and the covariance matrix for the class $i$. According to the Bayesian classifier, the decision function of LDA can be simplified as:

$$g(\mathbf{x}, i) = -\frac{1}{2}\mu_i^T\Sigma^{-1}\mu_i + \mathbf{x}^T\Sigma^{-1}\mu_i + \ln p(\omega_i) \tag{9}$$

where $\ln p(\omega_i)$ is the prior probability of class $\omega_i$. It generally assumes the prior probability is the same and homoscedastic for all actions in gesture recognition, i.e. $\ln p(\omega_i)$ is the same for each class and can be ignored in classification. The pooled covariance matrix $\Sigma$ is calculated as the average covariance matrixes of all classes. As a result, $\mu_i$ and $\Sigma_i$ are the only parameters in LDA, where $i = 1, 2, ...c$ and $c$ is the number of classes. A sample $\mathbf{x}$ is assigned to the class $i$ if $g(\mathbf{x}, i) > g(\mathbf{x}, j)$ where $j \neq i$, and $1 \leq j, i \leq c$.

### 2.6. Genetic Algorithm for Channel Selection

#### 2.6.1. Chromosome encoding

Binary encoding is used in this study to present the channel combinations, and thus the chromosomes is a string of bits (0 or 1). 0 indicates the corresponding channel that is not selected, while 1 indicates selecting the channel. We define $C_i$ as the state of the channel $i$. $C_i = 1$ indicates to select channel $i$, while $C_i = 0$ indicates not to select channel $i$. $\sum_{i=1}^{16} C_i = N$ indicates $N$ channels are selected in the chromosome. Fig. 4 demonstrates a chromosome that indicates $C_1 = 0$, $C_2 = 1$, $C_3 = 0$, $C_4 = 1$, $C_5 = 0$, $C_6 = 1$, $C_7 = 0$, $C_8 = 1$, $C_9 = 1$, $C_{10} = 0$, $C_{11} = 1$, $C_{12} = 1$, $C_{13} = 0$, $C_{14} = 0$, $C_{15} = 0$, $C_{16} = 1$.

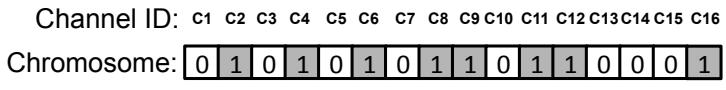


Figure 4. The binary encoding of a chromosome with channel 2, 4, 6, 8, 9, 11, 12, 16 selected.

### 2.6.2. Crossover and mutation

Single point crossover is adopted in this studies to generate the new offsprings. One crossover point is randomly generated before crossover. Two parent chromosomes (i.e. Chromosome A and B) generate two child chromosomes (i.e. Chromosome A+B and Chromosome B+A). A+B contains the gens from the beginning to the crossover point of A, and the gens from the crossover point to the end of B. Similarly, B+A contains the gens from the beginning to the crossover point of B, and the gens from the crossover point to the end of A. This study adopts bit inversion that selects one bit in a child chromosome after crossover, and inverses it under a given possibility ($p$), as demonstrated in Fig. 5.

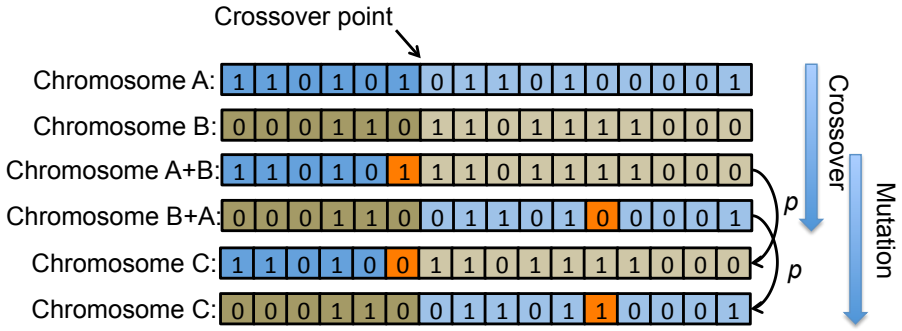


Figure 5. Crossover and mutation to generate new chromosomes.

### 2.6.3. Abnormal chromosome remover

When it is decided to select certain number of channels from 16 channels (i.e. $\sum_{i=1}^{16} C_i = N$), crossover and mutation would generate offsprings that may contain more or less channels than the requirement (i.e. $\sum_{i=1}^{16} C_i not = N$). Therefore, only the normal chromosome that contains required channel number will be put into the population pool of the new generation.

### 2.6.4. Algorithm implementation

Algorithm 1 demonstrates the implementation of the genetic algorithm for channel selection, in which the size of population is set to 50, and 10 best chromosomes are selected to generate offsprings. The possibility of mutation is set to 0.9 in the current study. The fitness is the 10-fold validation accuracy by a LDA classifier. The algorithm finishes when the selected ten best chromosomes are the same as the chromosomes of their parents. The inputs of the algorithms are samples of one subject, and the number of channels. The return values contain the best 10

chromosomes ($Chr$) as well as the corresponding accuracies ($Chr_{acc}$).

**Algorithm 1** Genetic algorithm for channel selection

```
procedure GenAlg(Samples, N)
    Randomly initialise 50 chromosomes
    Initialise Previous_Chr to zero matrix
    Select the 10 best chromosomes (Chr) according to the fitness
    while Previous_Chr ≠ Chr do
        Previous_Chr ← Chr
        Put the 10 best chromosomes into the population of next generation
        while The population of next generation does not reach 50 do
            Randomly select two chromosomes from Chr
            Generate two child chromosomes via crossover and mutation (p = 0.9)
            if One or two child chromosome(s) is normal then
                Put the normal child chromosome(s) into the population
        Select the 10 best chromosomes (Chr) according to the fitness
    return Chr, Chr_acc                    ▷ Chr_acc is the fitness (i.e. accuracy)
```

### 2.7. Metrics

- The hand gesture classification accuracy ($acc$) is defined as the following equation,

$$acc = \frac{T}{N}, \tag{10}$$

  where $N$ indicates the total number of predictions, and $T$ means the number of correct predictions. The function for the calculation of the accuracy is also regarded as the fitness function of the proposed genetic algorithm.
- The classification $acc$ is also

## 3. Results

### 3.1. How hand motion accuracy change with the number of sEMG channels

For the classification of thirteen hand gestures, the classification accuracies logarithmically grows with the increase number of selected sEMG channel for both optimally selection and random selection cases, as demonstrated in Fig. 7, . According to the experimental results, a fitting curves could be obtained as

$$y = 0.12\ln(x) + 0.48, \tag{11}$$

and

$$y = 0.14\ln(x) + 0.41 \tag{12}$$

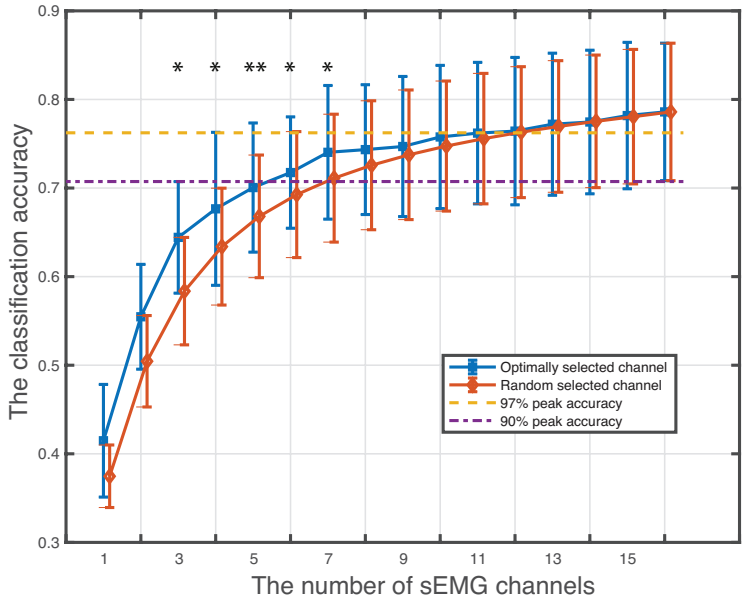


Figure 6. A comparison of accuracies between optimally selected channel and randomly selected channel. The error bar indicates the standard deviation across six subjects. Statistical analysis results comparing two channel selection approaches are shown above the corresponding number of channels, where sign * donates $p < 0.05$ and sign ** donates $p < 0.005$.

for optimally and random selection approach, with coefficient of determination of 0.93, and 0.97 respectively. The top accuracy of 78.59% was achieved when all sixteen channels were selected, while the lowest accuracy of only 37.47% could be obtained when randomly select one channel from sixteen channels. To reach 97% of the maximum accuracy using all 16 sEMG channels, the experiments about 12 channels should be selected, no matter in optimal or random approach. To reach more than 90% of the maximum accuracy, at least six channels need to be optimally selected, but at least seven channels are required for random channel selection approach. It was also found that the accuracy improvement by the optimal approach was much obvious when only a few channels (i.e. $< 8$) were required to be selected. Statistical analysis demonstrated that the improvement were significant ($p < 0.05$, paired t-test) when only 3, 4, 5, 7 or 8 channels were required.

The channel selection approaches were also evaluated in the classification of different groups of hand gestures. The experiments divided the hand gestures into three subgroup of gestures: basic gestures, wrist gesture, and grasp gestures. $HR$, $HC$ and $HO$ were included in basic gestures. $WF$, $WE$, $WP$, $WS$, $UF$, and $RF$ were grouped into wrist gestures. The experimental results were given in Fig. 7.

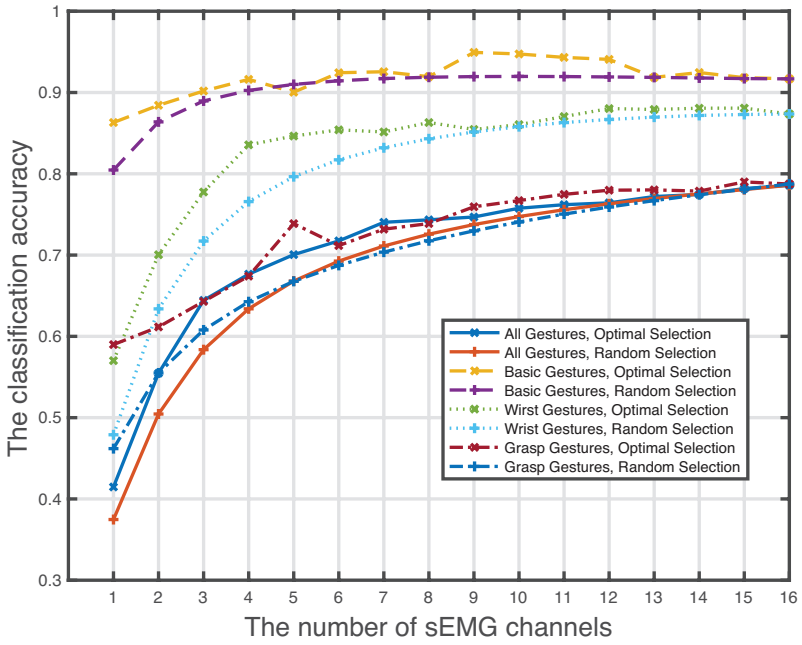


Figure 7. A comparison of the effects of channel optimisation for different groups of hand gestures.

The classification accuracy for three basic hand gestures when using all 16 channels were more than 90%, that was around 5% higher than that of classifying six wrist gestures. The accuracies of classifying all the thirty gestures were similar with that of classifying four grasp gestures, which were a little bit lower than 80%. Statistical analysis demonstrated that the optimal solution was not significantly ($p < 0.05$) better than random selection solution, when classifying three basic hand gestures. However, for classifying the wrist gestures, optimal selection approach significantly outperformed ($p < 0.05$) random selection approach when using 1 to 8 channels of sEMG signals. The statistically significant improvement was also identified when classifying four grasp gestures, but only for 1, 4, 5 channels of sEMG signals. In sum, similar performance could be found when classifying different groups of hand gestures, and optimal selection generally outperformed random selection, especially when the required channel numbers were less than eight channels.

### 3.2. Which channels can be selected?

Except for the investigating of the relation between hand motion classification accuracies and the utilised number of channels, this study also concerned whether there exists certain channels that could consistently provide effective sEMG sig-

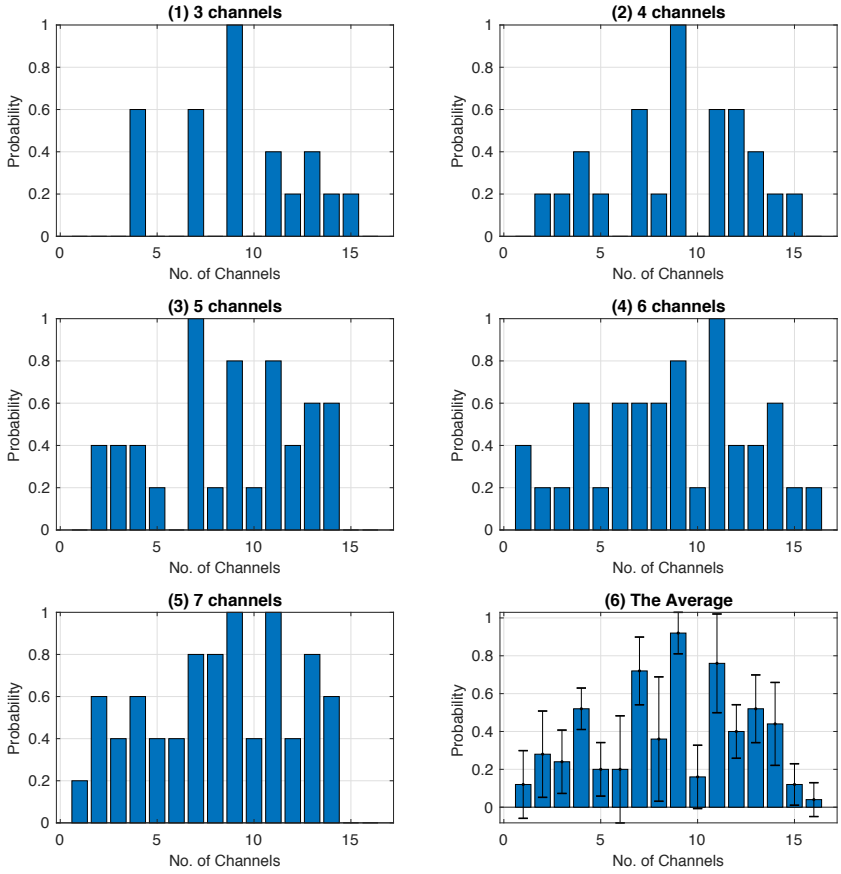


Figure 8. The statistical results of the selected channels across six subjects, where the total number of 3, 4, 5, 6 and 7 channels are concerned, as represented in subfigures (1), (2), (3), (4), and (5), respectively. The height of each bar indicates the probability that the corresponding channel was preferred for six tested subjects. Subfigure (6) demonstrates the averaged probability for the above five cases, where the error indicates the standard deviations.

nals. According to the previous experimental results, optimally selecting three to seven channels could achieve statistically significant improvement against random selection, and thus three to seven channels were taken into consideration in the following experiments.

Firstly, it was not found that the selected channels from different subjects were consistent, but there did exist several channels that could provide better signal against others. As demonstrated in Figs. 8 (1), (2) and (5), channel 9 were consistently selected for all subjects. Channel 7 were also consistently selected in Figs. 8 (3) and (4). As the overall results demonstrated in Fig. 8 (6), channel 9 owned

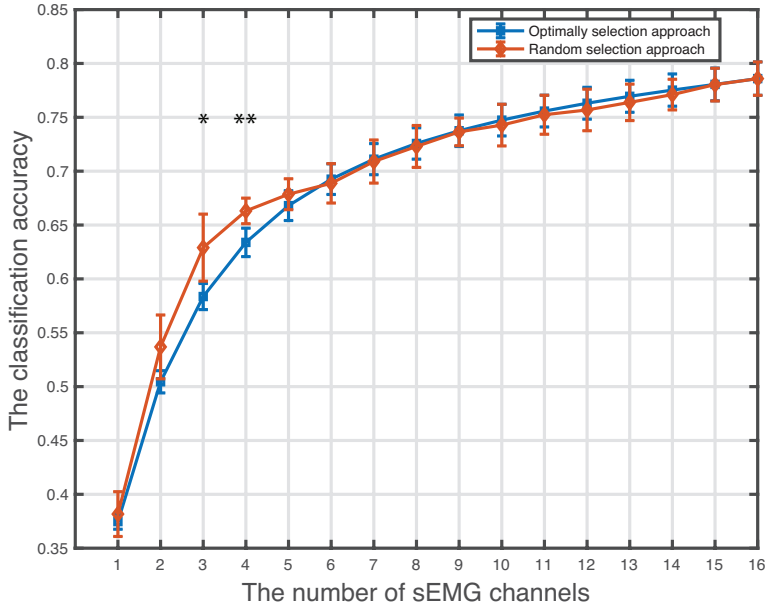


Figure 9. A comparison of cross-validation accuracies between optimally selected channels and randomly selected channels. The error bar indicates the standard deviation across six subjects. Statistical analysis results comparing two channel selection approaches are shown above the corresponding number of channels, where sign * donates $p < 0.05$ and sign ** donates $p < 0.005$.

the highest probability to be selected, which was statistically significant ($p < 0.05$) against the other channels expect channel 7 and 11.

### 3.3. Cross-validation

The cross subject validation results are demonstrated in Fig.9. The same as cross-day-validation results demonstrated in Fig. 6, the classification accuracies logarithmically grows with the increase number of selected sEMG channel for both optimally and random channel selection apporach. According to the experimental results, a fitting curves could be obtained as

$$y = 0.13\ln(x) + 0.44, \tag{13}$$

for optimally selection approach with the coefficient of determination of 0.94. It was clearly demonstrated that optimally selecting channel could function when only two to four channels were required to be selected, and our statistical analysis showed that the improvements were significant ($p < 0.05$) when the number of channels were three and four. The accuracy improved from 58.4% to 62.9% by 4.5%, and

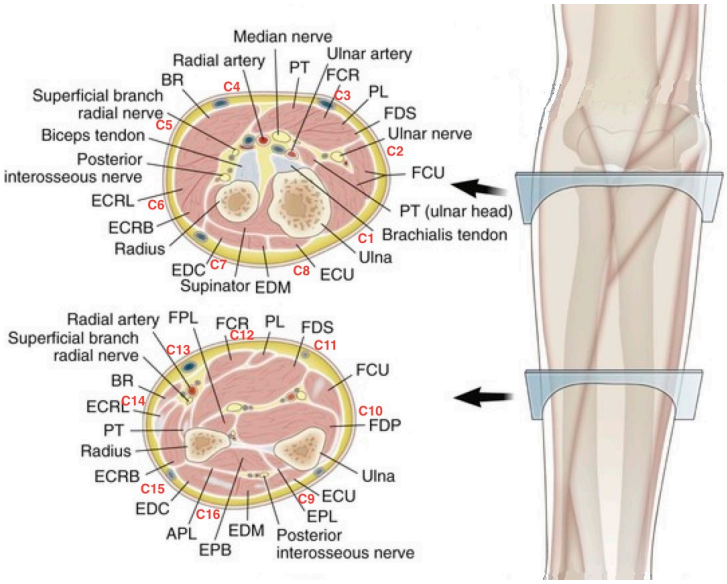


Figure 10. Cross-sectional anatomy at the level proximal forearm and mid forearm. C1 to C16 indicate the rough position of the sEMG channel corresponding to the forearm muscle. APL, Abductor pollicis longus; BR, brachioradialis; ECRB, extensor carpi radialis brevis; ECRL, extensor carpi radialis longus; ECU, extensor carpi ulnaris; EDC, extensor digitorum communis; EDM, extensor digiti minimi; EIP, extensor indicis proprius; EPB, extensor pollicis brevis; EPL, extensor pollicis longus; FCR, flexor carpi radialis; FCU, flexor carpi ulnaris; FDP, flexor digitorum profundus; FDS, flexor digitorum superficialis; FPL, flexor pollicis longus; PL, palmaris longus; PQ, pronator quadratus; PT, pronator teres.

from 63.4% to 66.3% by 4.5% when only three and four channels were required to be selected. In terms of which three or four channels should be selected, as already demonstrated in Fig. 8, the most suitable combination for three and four channels were channels [4, 7, 9] and [4, 9, 11, 12], respectively.

## 4. Discussion

In the current study, the optimally selected eleven channel can reach up to 97% the best performance, which is consistent with finding in[18], illustrating that twelve bipolar sEMG channel can reach 98.8% of the best performance when using the entire HD EMG map. The use of two sEMG channels to control the open, close state of a prothetic hand can guarantee the robustness, but it is far from being intuitive and smart. Therefore, the current study further confirms that, combining advanced machine-learning algorithm, eleven or twelve sEMG channels can be a good choice to fulfil a multi-functional MyoHMI.

Electrode shift is widely accepted to be the most negative factor influence hand gesture recognition accuracy. It is even significant for inter-day hand gesture recog-

nition, where electrode position may shift a lot during different wearings. As discussed by Boschman et al.[33], the use of sufficient sEMG channels can compensate slight electrode shift less than one cm, but more than 2-cm shift would completely deteriorate a classification system. Intuitively, the optimisation of electrode configuration is likely to mitigate the impact of electrode shift. As demonstrated in Fig. 8, the channels with the larger number (nine to sixteen) is preferred by the genetic algorithm. As can be found in Fig. 10, these electrode channels are located in the mid forearm. By the comparison of proximal and mid forearm anatomy, mid forearm may provide more rich information on muscular actives from different muscles. It is because the sEMG signal captured from the proximal forearm may be dominated by the flexor and extensor and the deep muscle activities are less reflected, but these deep muscles may become shallow in the mid forearm. In sum, placing electrode on the mid forearm is more likely to provide rich information for inter-day hand gesture recognition, despite the difficulty of electrode positioning on the slope of the forearm.

## 5. Conclusion

The current study adopted genetic algorithm to implement the sEMG channel optimisation task for inter-day hand gesture recognition accuracy. A sEMG dataset was recorded for the experiments. An genetic algorithm were specially developed for sEMG channel optimisation, including the chromosome encoding, crossover and mutation, abnormal chromosome remover. The experimental results disclosed that 1) the use of eleven sEMG channels can reach 97% of the best performance on inter-day gesture recognition; 2) placing the electrodes on the mid forearm can achieve better performance than on the proximal forearm; 3) The optimised channel combination by genetic algorithm could improve the accuracy by more than 3% in the comparison with the baseline, which was verified by cross-validation test.

## 6. Acknowledgments

The contribution was funded by the 7th framework programme of the European Union (Grant No. 600915).

## Bibliography

1. D. Farina, S. Member, N. Jiang, H. Rehbaum, S. Member, A. Holobar, B. Graimann, H. Dietl, and O. C. Aszmann, “The Extraction of Neural Information from the Surface EMG for the Control of Upper-Limb Prostheses : Emerging Avenues and Challenges,” IEEE Trans. Neural Syst. Rehabil. Eng., vol. 22, no. 4, pp. 797–809, 2014.
2. B. Hudgins, P. Parker, and R. N. Scott, “A new strategy for multifunction myoelectric control,” IEEE Trans. Biomed. Eng., vol. 40, no. 1, pp. 82–94, 1993.
3. Y. Fang, D. Zhou, K. Li, and H. Liu, “Interface Prostheses with Classifier-Feedback based User Training,” IEEE Trans. Biomed. Eng., vol. 64, no. 11, pp. 2575–2583, 2017.
4. Z. Ju, G. Ouyang, M. Wilamowska-Korsak, and H. Liu, “Surface emg based hand

manipulation identification via nonlinear feature extraction and classification," IEEE Sensors J., vol. 13, no. 9, pp. 3302–3311, 2013.
5. Y. Sun, C. Li, G. Li, G. Jiang, D. Jiang, H. Liu, Z. Zheng, and W. Shu, "Gesture recognition based on kinect and semg signal fusion," Mobile Networks and Applications, pp. 1–9, 2018.
6. X. Chen, D. Zhang, and X. Zhu, "Application of a self-enhancing classification method to electromyography pattern recognition for multifunctional prosthesis control," J Neuroeng Rehabil., vol. 10, no. 1, p. 44, 2013.
7. S. Li, J. He, X. Sheng, H. Liu, and X. Zhu, "Synergy-driven myoelectric control for emg-based prosthetic manipulation: A case study," Int. J. Humanoid Robotics, vol. 11, no. 02, p. 1450013, 2014.
8. R. Menon, G. Di Caterina, H. Lakany, L. Petropoulakis, B. A. Conway, and J. J. Soraghan, "Study on interaction between temporal and spatial information in classification of emg signals for myoelectric prostheses," IEEE Trans. Neural Syst. Rehabil. Eng., vol. 25, no. 10, pp. 1832–1842, 2017.
9. Y. Du, W. Jin, W. Wei, Y. Hu, and W. Geng, "Surface EMG-Based Inter-Session Gesture Recognition Enhanced by Deep Domain Adaptation," Sensors, pp. 6–9, 2017.
10. W. Geng, Y. Du, W. Jin, W. Wei, Y. Hu, and J. Li, "Gesture recognition by instantaneous surface EMG images," Sci. Rep., vol. 6, no. 1, p. 36571, 2016.
11. H. Daley, K. Englehart, L. Hargrove, and U. Kuruganti, "High density electromyography data of normally limbed and transradial amputee subjects for multifunction prosthetic control," J. Electromyogr. Kines., vol. 22, no. 3, pp. 478–84, 2012.
12. C. L. Pulliam, J. M. Lambrecht, and R. F. Kirsch, "Electromyogram-based neural network control of transhumeral prostheses," J. Rehabil. Res. Dev., vol. 48, no. 6, pp. 739–54, 2011.
13. A. Fougner, E. Scheme, A. D. Chan, K. Englehart, and O. Stavdahl, "A multi-modal approach for hand motion classification using surface emg and accelerometers," Conf. Proc. IEEE Eng. Med. Biol. Soc., vol. 2011, pp. 4247–50, 2011.
14. S. Muceli and D. Farina, "Simultaneous and proportional estimation of hand kinematics from emg during mirrored movements at multiple degrees-of-freedom," IEEE T. Syst. Rehabil. Eng., vol. 20, no. 3, pp. 371–8, 2012.
15. R. N. Khushaba, A. Al-Ani, and A. Al-Jumaily, "Orthogonal fuzzy neighborhood discriminant analysis for multifunction myoelectric hand control," IEEE Trans. Biomed. Eng., vol. 57, no. 6, pp. 1410–9, 2010.
16. F. Tenore, A. Ramos, A. Fahmy, S. Acharya, R. Etienne-Cummings, and N. V. Thakor, "Towards the control of individual fingers of a prosthetic hand using surface emg signals," Conf. Proc. IEEE Eng. Med. Biol. Soc., vol. 2007, pp. 6146–9, 2007.
17. A. J. Young, L. J. Hargrove, and T. A. Kuiken, "Improving myoelectric pattern recognition robustness to electrode shift by changing interelectrode distance and electrode configuration," IEEE Trans. Biomed. Eng., vol. 59, no. 3, pp. 645–652, 2012.
18. H. He, Z. Ping, L. Guanglin, and T. A. Kuiken, "An analysis of emg electrode configuration for targeted muscle reinnervation based neural machine interface," IEEE Trans. Syst. Rehabil. Eng., vol. 16, no. 1, pp. 37–45, 2008.
19. Y. Fang, N. Hettiarachchi, D. Zhou, and H. Liu, "Multi-modal sensing techniques for interfacing hand prostheses: a review," IEEE Sens. J., vol. 15, no. 11, pp. 6065–6076, 2015.
20. C. Castellini and P. V. D. Smagt, "Surface emg in advanced hand prosthetics," Biol. Cybern., vol. 100, no. 1, pp. 35–47, 2009.
21. U. Baspinar, H. S. Varol, and V. Y. Senyurek, "Performance comparison of artificial neural network and gaussian mixture model in classifying hand motions by using semg

signals," Biocybern. Biomed. Eng., vol. 33, no. 1, pp. 33–45, 2013.
22. N. M. Kakoty and S. M. Hazarika, "Recognition of grasp types through principal components of dwt based emg features," IEEE Int. Conf. Rehabil. Robot, vol. 2011, p. 5975398, 2011.
23. C. Castellini, E. Gruppioni, A. Davalli, and G. Sandini, "Fine detection of grasp force and posture by amputees via surface electromyography," J. Physiol. Paris., vol. 103, no. 3-5, pp. 255–62, 2009.
24. G. Huang, Z. Zhang, D. Zhang, and X. Zhu, "Spatio-spectral filters for low-density surface electromyographic signal classification," Med. Biol. Eng. Comput., vol. 51, no. 5, pp. 547–55, 2013.
25. G. Drost, D. F. Stegeman, B. G. van Engelen, and M. J. Zwarts, "Clinical applications of high-density surface emg: a systematic review," J. Electromyogr. Kines., vol. 16, no. 6, pp. 586–602, 2006.
26. D. Zhou, Y. Fang, N. Kubota, and H. Liu, "Surface EMG based hand motion recognition using combined growing neural gas and linear discriminant analysis," in 10th International Conference on Human System Interaction (HSI2017). IEEE, 2017.
27. M. A. Oskoei and H. Hu, "GA-based feature subset selection for myoelectric classification," 2006 IEEE International Conference on Robotics and Biomimetics, ROBIO 2006, pp. 1465–1470, 2006.
28. Y. Fang, X. Zhu, and H. Liu, "Development of a surface emg acquisition system with novel electrodes configuration and signal representation," in Proc. Int. Conf. Intel. Rob. Appl. Springer, 2013, pp. 405–414.
29. Y. Fang, H. Liu, G. Li, and X. Zhu, "A multichannel surface emg system for hand motion recognition," Int. J. Humanoid Robotics, vol. 12, no. 02, p. 1550011, 2015.
30. Y. Fang and H. Liu, "Robust semg electrodes configuration for pattern recognition based prosthesis control," in Systems, Man and Cybernetics (SMC), 2014 IEEE International Conference on. IEEE, 2014, pp. 2210–2215.
31. Y. Fang, "Interacting with prosthetic hands via electromyography signals," Ph.D. dissertation, University of Portsmouth, 2015.
32. K. Englehart and B. Hudgins, "A robust, real-time control scheme for multifunction myoelectric control," IEEE Trans. Biomed. Eng., vol. 50, no. 7, pp. 848–854, 2003.
33. A. Boschmann and M. Platzner, "Reducing classification accuracy degradation of pattern recognition based myoelectric control caused by electrode shift using a high density electrode array," in Conf. Proc. IEEE Eng. Med. Biol. Soc. IEEE, 2012, pp. 4324–4327.

Zheng Wang received the B.S. in Biological Engineering from Zhejiang University of Technology in 2009 and the M.S. degree in Computational Biology from University of East Anglia in 2012. He is currently a Phd candidate in Control Science at Zhejiang University of Technology, and he also holds a lecture position in Zhejiang institute of Mechanical and Electrical Engineering.

Zheng Wang has published over 10 journal and conference papers. His research insterest includes Intelligent Computing and Intelligent Systems, Complex logistics

system optimization dispatch and artificial intelligence.

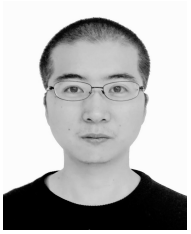

Yinfeng Fang received the Ph.D. degree from University of Portsmouth in 2015. He received the B.S. degree in Electrical and Information Engineering and the M.S. degree in Pattern Recognition and Intelligent System from the Zhejiang University of Technology, China, in the year 2005 and 2009, respectively. He is currently a Senior Research Associate in the Intelligent System and Biomedical Robotics group at the University of Portsmouth.

Yinfeng Fang is the author of over 20 peer-reviewed journal and conference papers. His research interests include bioelectric signals acquisition electronics (analog and digital), signal processing and artificial intelligence algorithms for pattern recognition and control, neuromuscular interfaces, virtual and augmented reality for neuromuscular rehabilitation.

Honghai Liu received his Ph.D degree from King's College London, UK. He is a Chair in intelligent systems at the School of Computing, the University of Portsmouth, UK. He previously held research appointments at the Universities of London, University of Aberdeen, and project leader appointments in large-scale industrial control and system integration industry. His research has been funded by UK research councils, EU FP7, the Leverhulme Trust, the Royal Society and industry partners.

Honghai Liu is the author of over 200 technical publications, proceedings editorials and books. He is also the Co-Editor-in-Chief for the Springer Journal of Intelligent Robotics and Applications and Associate Editor for IEEE Transactions on Industrial Electronics and IEEE Transactions on Industrial Informatics. He is interested in intelligent sensing, biomechatronics, pattern recognition, intelligent video analytics, intelligent robotics and their practical applications with an emphasis on approaches that could make contribution to the intelligent connection of perception to action using contextual information.